Multipole oscillations in sodium clusters: Separable ansatz in the random-phase-approximation description

V. O. Nesterenko, W. Kleinig,* and V. V. Gudkov
Bogoliubov Laboratory of Theoretical Physics, Joint Institute for Nuclear Research, 141980 Dubna, Moscow Region, Russia

N. Lo Iudice
Università di Napoli ''Federico II'' and Dipartimento di Scienze Fisiche, Istituto Nazionale di Fisica Nucleare, Mostra d'Oltremare Padiglione 19, I-80125 Napoli, Italy

J. Kvasil
Department of Nuclear Physics, Charles University, CS-18000, Prague, Czech Republic
(Received 11 November 1996)

The modified random-phase-approximation (RPA) method with the self-consistent *separable* residual forces (SRPA) is proposed for the description of multipole electric oscillations of valence electrons in sodium clusters. The method allows one to study the coupling of different kinds of collective motion. As a particular case, the coupling of surface and volume modes is considered. The SRPA is applied to neutral and singly charged spherical sodium clusters in a wide size region ($N_e = 8,20,40,58,92,138,196,440,952$) and good agreement with experimental data is achieved. This testifies to the applicability of the separable ansatz, which has the essential advantage of avoiding diagonalization of the RPA matrices and thus drastically simplifies the RPA calculations. The latter could be quite urgent for very large and deformed clusters where an extended configuration space and, consequently, high-rank RPA matrices are used. The predictions for $E2$ and $E3$ collective excitations are presented. The results obtained with the self-consistent Kohn-Sham and phenomenological Woods-Saxon single-particle schemes are exhibited and different parameters for the Woods-Saxon potential are proposed. [S1050-2947(97)06906-0]

PACS number(s): 36.40.Gk, 36.40.Vz

I. INTRODUCTION

Collective oscillations in metal clusters, mainly the surface dipole plasmon, are now a field of intensive investigation (see reviews [1–5]). These modes have been widely studied in different random-phase-approximation (RPA) approaches [2–4,6–16]. RPA methods provide a mechanism that accounts naturally for the Landau damping, a phenomenon that is known to affect considerably the dipole plasmon. This is in fact explained as a fragmentation of the collective strength over particle-hole excitations.

A large variety of the RPA methods, all being based on the linearization of the equations of motion, are available. The hierarchy of different RPA versions can be found in reviews [14]. The simplest version is based on a sum-rule approach and is valid only if most of the collective strength is concentrated in one dominant peak [13,17–19]. This is not the case for dipole oscillations in deformed and even some spherical clusters such as Na_{20} (for sodium clusters see Refs. [20–23]). A more correct description is provided by the local RPA [14,19,24], where as many collective peaks as the number of introduced local operators (usually 4–10) can be studied. This method accounts for the gross features of the collective strength distribution, but is unable to describe the Landau damping. To this aim, more elaborate RPA methods (full RPA) have been used successfully. They are known as the time-dependent local-density approximation (TDLDA), the time-dependent Hartree-Fock approximation, the discrete-matrix RPA, etc. [6–12]. Within the TDLDA, for instance, the photoabsorption and photoemission of neutral spherical sodium clusters in a wide region have been described as early as 1985 [6]. Nowadays, full RPA methods are the most powerful theoretical instruments for the description of collective excitations in metal clusters. In dealing with these methods, however, one has to solve a system of eigenvector equations whose rank equals the number of basic particle-hole configurations. This is not a problem if we study spherical clusters of a moderate size. However, we can run into serious computational troubles in the cases of large spherical clusters and especially of deformed clusters, for which an impressively large configuration space is required.

This drawback can be overcome by resorting to the self-consistent schematic RPA (SRPA) method, otherwise called the vibrating potential model [13,15,16,25,26]. Within this approach a *separable* residual two-body interaction is derived. Such a separable ansatz allows one to turn the RPA matrix into a dispersion relation that drastically simplifies the eigenvalue problem. At the same time, the SRPA enables us to treat the Landau damping as in the full RPA. The validity of the separable approximation has been analytically proved for short-range interactions [27]. In practice, its range of applicability is much wider. In particular, it was successfully used for long-range (in nuclear scale) nuclear forces in many studies of collective excitations in atomic nuclei [25–29]. In metal clusters, we deal with the long-range screened Coulomb interaction. It is therefore difficult to assert from the

*Permanent address: Technical University Dresden, Institute for Analysis, D-01062, Dresden, Germany.

very beginning or to prove analytically the applicability of the separable ansatz. Only full-scale calculations can provide an answer to this question.

The aim of this paper is to present the self-consistent version of the SRPA and to show that this approach provides a good description of dipole oscillations in sodium clusters. The method will be used to study both neutral and singly charged ($Z=+1$) spherical sodium clusters in a wide region ($N_e=8-952$). Spherical clusters, being well studied both experimentally and theoretically, are a good test ground for the method. It should be mentioned that SRPA calculations recently performed for *deformed* clusters [30] yielded results in good agreement with experiments [31]. Moreover, SRPA and full RPA [32] results obtained with the same energy functional seem to be very close. This may be already considered as a proof of the applicability of the separable ansatz for the description of dipole oscillations in sodium clusters.

The time-dependent version of the SRPA for metal clusters has been proposed in Ref. [13] and subsequently generalized to the case of deformed clusters [33]. First numerical calculations for a dipole plasmon in both spherical and deformed neutral sodium clusters were made [15,16]. In Ref. [16], the Woods-Saxon single-particle scheme and *surface* self-consistent separable residual interaction were used. The results obtained were encouraging. However, without explicit treatment of the ionic subsystem [4], the calculations [16], like many other RPA methods, overestimate to some extent the energy of the surface plasmon, especially in small clusters. Starting from $N_e>20$ (N_e is the number of valence electrons), a too-strong high-energy strength was also predicted. For example, for Na_{26} and Na_{40}, the computed dipole strength at energies $E>3.4$ eV exhausts 30% and 44%, respectively, while the experimental data [20,21] give 10–15% for clusters of this size and up to 20–30% for larger clusters [34]. So strong high-energy strength is not supported by either local and full RPA calculations (see, e.g., [12,35]). A total blueshift of the dipole strength obtained in [16] leads to a considerable underestimation of the static dipole polarizabilities. In order to prove the applicability of the SRPA for sodium clusters, we certainly have to overcome these shortcomings.

In the present paper we will considerably improve the description of dipole oscillations by (a) using the Kohn-Sham single-particle scheme with a diffused jellium and (b) taking into account the coupling of the surface and volume degrees of freedom [36]. The diffuseness of the jellium simulates a pseudopotential folding [37] and, as shown below, leads to the redshift of the surface plasmon energy in close agreement with the experimental value. Following the local RPA prescription [19], the coupling of the surface and volume dipole modes is included to decrease the high-energy strength. As shown below, such a coupling considerably improves the description of the dipole oscillations. Here we have a close analogy to the counterpart of the dipole plasmon in atomic nuclei, the dipole giant resonance, which is also best described when volume (Steinwedel-Jensen model [38]) degrees of freedom are coupled to the dominant surface (Goldhaber-Teller model [39]) degrees [40,41]. The improvements mentioned above allow one to get good agreement with the available experimental data, thereby providing solid ground for the separable approximation.

As compared with the previous versions [13,15,16,33], the SRPA is generalized so as to take simultaneously into account different kinds of collective motion. Although in the present paper a particular case of the coupling of surface and volume modes is considered, the present model, being of quite general character, can be used also to study the coupling of other collective degrees of freedom. As shown below, different kinds of collective motion are introduced through the set of input local operators. The generalized SRPA covers both the previous SRPA versions [13,15,16,33] and the local RPA [19,24] as the particular cases. While the local RPA can be treated as a system of coupled oscillators where the number of the oscillators is equal to the number of input local operators, the generalized SRPA represents a system of coupled collective motions, each one being described within the RPA. Like in the local RPA, the number of different kinds of collective motions is equal to the number of input local operators. However, the total number of excitations in the generalized SRPA is determined by the number of particle-hole configurations of a given multipolarity. If one considers a single kind of collective motion (one local operator), we have the previous SRPA, and vice versa, if only the most collective RPA state is retained for every collective motion, we obtain the local RPA description.

The calculations have been performed using the self-consistent diffused Kohn-Sham [42,43] and phenomenological Woods-Saxon single-particle schemes. It will be shown that the Woods-Saxon potential, in spite of appreciable deviations of its behavior from the Kohn-Sham scheme in the surface region, is, nevertheless, quite acceptable for the study of the dipole dynamical response. Alternative parameters for the Woods-Saxon potential, providing a good description of the surface plasmon in a wide region, are proposed for both neutral and charged clusters.

II. MAIN SRPA EQUATIONS

The simplest form of a separable two-body interaction is [25–27]

$$\sum_{p_1,p_2,h_2,h_1} V(p_1,p_2,h_2,h_1) = \kappa \sum_{p_1,p_2,h_2,h_1} q(p_1,h_1)q(p_2,h_2), \qquad (1)$$

where $q(p_1,h_1)$ are single-particle (particle-hole) matrix elements of one-body operators. By directly making this ansatz, however, we do not obtain any prescription for determining the strength constant κ and the structure of the one-body operator (in the linear response theory, this operator should be equal to the external field operator, i.e., in general, it is not consistent with the mean field). A more effective way is provided by the time-dependent formulation of the SRPA proposed for metal clusters in Refs. [13,16,33]. This approach leads to the same dispersion equations for the excitation energies, but, at the same time, provides the expressions for the strength constant and self-consistent operator of residual forces. As a result, the method itself does not need any adjusting parameters.

Let us present the SRPA derivation for a general case when not one but several kinds (for example, surface and volume) of collective motions of a given multipolarity are taken into account simultaneously. We start with the Kohn-Sham energy functional for a system of N_e valence electrons

$$E\{n(\mathbf{r},t),\tau(\mathbf{r})\} = \frac{1}{2}\int \tau(\mathbf{r},t)d\mathbf{r} + \int v(n(\mathbf{r},t))d\mathbf{r} + \frac{1}{2}\int\int \frac{[n(\mathbf{r},t)-n_i(\mathbf{r})][n(\mathbf{r}_1,t)-n_i(\mathbf{r}_1)]}{|\mathbf{r}-\mathbf{r}_1|}d\mathbf{r}\,d\mathbf{r}_1, \tag{2}$$

which includes the kinetic energy, the exchange-correlation term in the local density approximation [44], and the Coulomb term, respectively. Here $n(\mathbf{r},t)=\Sigma_l|\phi_l(\mathbf{r},t)|^2$ and $\tau(\mathbf{r},t)=\Sigma_l|\nabla\phi_l(\mathbf{r},t)|^2$ are the density and kinetic-energy density of valence electrons, $n_i(\mathbf{r})$ is the ionic density in the jellium approximation, and $\phi_l(\mathbf{r},t)$ is a single-particle wave function. The expression for the exchange-correlation term $v(n(\mathbf{r},t))$ is given in Sec. III. The convention $e=m_e=\hbar=1$ is used.

The time-dependent single-particle Hamiltonian is obtained as

$$H(\mathbf{r},t)\phi_l(\mathbf{r},t)=\frac{\delta E}{\delta\phi_l^*(\mathbf{r},t)}. \tag{3}$$

In the small-amplitude limit of collective motion, it is written as a sum of the static

$$H_0(\mathbf{r})=-\frac{\Delta}{2}+\left(\frac{dv}{dn}\right)_{n=n_0}+\int\frac{n_0(\mathbf{r}_1)-n_i(\mathbf{r}_1)}{|\mathbf{r}-\mathbf{r}_1|}d\mathbf{r}_1 \tag{4}$$

and dynamic parts

$$\delta H(\mathbf{r},t)=\left(\frac{d^2v}{dn^2}\right)_{n=n_0}\delta n(\mathbf{r},t)+\int\frac{\delta n(\mathbf{r}_1,t)}{|\mathbf{r}-\mathbf{r}_1|}d\mathbf{r}_1, \tag{5}$$

where $n(\mathbf{r},t)=n_0(\mathbf{r})+\delta n(\mathbf{r},t)$, $n_0(\mathbf{r})$ is the static ground-state density, and $\delta n(\mathbf{r},t)$ is a small-amplitude time-dependent density variation (transition density). Equation (4) constitutes the Kohn-Sham single-particle potential.

To determine the density variation corresponding to the excitations of multipolarity $\lambda\mu$, we should first define the perturbed time-dependent wave function of the system. It is convenient to do this through the scaling transformation

$$\Psi_j(\mathbf{r}_1,\ldots,\mathbf{r}_{N_e},t) = \prod_{k=1}^{K}\exp\left(i\alpha_{\lambda\mu k}^j(t)\sum_{l=1}^{N_e}[H_0(\mathbf{r}_l),f_{\lambda\mu k}(\mathbf{r}_l)]\right) \times\Psi_0(\mathbf{r}_1,\ldots,\mathbf{r}_{N_e}), \tag{6}$$

where Ψ_0 is the ground-state wave function ($H_0\Psi_0=0$) and j labels the roots of the dispersion equation. Both Ψ_0 and Ψ_j are Slater determinants.

The local Hermitian coordinate operators $f_{\lambda\mu k}(\mathbf{r})$ determine the kinds of collective motion provided by the density variation. They influence the residual interaction and thus the eigenstates and eigenenergies of the system. So they should not be confused with an external field operator used in the linear-response theory. For the reasons given below, these operators are chosen as $f_{\lambda\mu k}(\mathbf{r})=r^{p_k}[Y_{\lambda\mu}(\theta,\phi)+Y_{\lambda\mu}^{\dagger}(\theta,\phi)]$, with $k=1,\ldots,K$. Further, $\alpha_{\lambda\mu k}^j(t)=\alpha_{\lambda\mu k}^{j0}\cos(\omega t)$ are harmonic collective variables. Their normalized amplitudes $\alpha_{\lambda\mu k}^{j0}$ account for the relative contributions to electron oscillations of different kinds of collective motion and, as shown below, are calculated from the final SRPA equations.

By virtue of Eq. (6), the density variation can be written in the form

$$\delta n_j(\mathbf{r},t)=\sum_{k=1}^{K}\alpha_{\lambda\mu k}^j(t)[\nabla n_0(\mathbf{r})\nabla f_{\lambda\mu k}(\mathbf{r})+n_0(\mathbf{r})\Delta f_{\lambda\mu k}(\mathbf{r})]. \tag{7}$$

It is seen to include both surface $\sim\nabla n_0(\mathbf{r})$ and volume $\sim n_0(\mathbf{r})$ terms. If $p_k=\lambda$, we have a divergency-free operator [$\Delta f_{\lambda\mu k}(\mathbf{r})=0$] and Eq. (7) has only the surface term. This case was considered in [16]. The operators with $p_k>\lambda$ are responsible for a volume collective motion: They produce a general shift of the total density variation (7) towards the interior of the system. As discussed in Sec. I, volume degrees of freedom for dipole excitations are important in both atomic nuclei and metal clusters. In [19], the set of local operators with $p_k=1,4,7,10,13$ was proposed. This was found to be the minimal set that could bring the calculation to converge toward the full RPA. In this connection, it is worth noting that in atomic nuclei the dipole excitations of volume character are described within the Steinwedel-Jensen model, where the spherical Bessel function $j_1(qr)$ plays the same role as the operators $f_{\lambda\mu k}(\mathbf{r})$ ($p_k>\lambda$) in the local RPA and SRPA. It is easy to see the correspondence between the polynomial expansion of the spherical Bessel function and the set of the local operators (in the dipole case, the operators with even p approximate the odd neighbors). Our study has shown that for the coupling of surface and volume modes the sets $p_k=1,4,7,10$, $p_k=2,4,6,8$, and $p_k=3,5,7,9$ are quite sufficient for describing dipole, quadrupole, and octupole oscillations, respectively. In principle, a good convergence of the SRPA results is reached already at $p_k=1,4$, $p_k=2,4$, and $p_k=3,5$ since, unlike the local RPA, the SRPA provides a rich spectrum of dipole excitations already for one local operator. Collective oscillations are in fact described as coherent superpositions of particle-hole configurations. The total number of states is therefore equal to the number of these elementary configurations. For this reason the SRPA does not need a large number of local operators.

Substituting Eq. (7) into (5), we have

$$\delta H(\mathbf{r},t)=\sum_{k=1}^{K}\alpha_{\lambda\mu k}^j(t)Q_{\lambda\mu k}(\mathbf{r}), \tag{8}$$

with

$Q_{\lambda\mu k}(\mathbf{r})$

$$=\left(\frac{d^2v}{dn^2}\right)_{n=n_0}[\nabla n_0(\mathbf{r})\nabla f_{\lambda\mu k}(\mathbf{r})+n_0(\mathbf{r})\Delta f_{\lambda\mu k}(\mathbf{r})]$$
$$+\int\frac{[\nabla n_0(\mathbf{r}_1)\nabla f_{\lambda\mu k}(\mathbf{r}_1)+n_0(\mathbf{r}_1)\Delta f_{\lambda\mu k}(\mathbf{r}_1)]}{|\mathbf{r}-\mathbf{r}_1|}d\mathbf{r}_1. \tag{9}$$

The first and second terms on the right-hand side of Eq. (9) are contributions of the exchange-correlation and direct Coulomb parts of the functional (2), respectively.

We now substitute the Hamiltonian $H(\mathbf{r},t)=H_0(\mathbf{r})+\delta H(\mathbf{r},t)$ into the time-dependent Hartree-Fock equation

$$\sum_{l=1}^{N_e}H(\mathbf{r}_l,t)\Psi_j(\mathbf{r}_1,\ldots,\mathbf{r}_{N_e},t)=i\frac{d}{dt}\Psi_j(\mathbf{r}_1,\ldots,\mathbf{r}_{N_e},t). \tag{10}$$

Following the Thouless theorem [45], the wave function of the system can be written in the form

$$\Psi_j(\mathbf{r}_1,\ldots,\mathbf{r}_{N_e},t)=\left(1+\sum_{ph}c^j_{ph}(t)\right)\Psi_0(\mathbf{r}_1,\ldots,\mathbf{r}_{N_e}), \tag{11}$$

where $c^j_{ph}(t)$ give the particle-hole contributions to the excited state. By linearization of Eq. (10), we get

$$\epsilon_{ph}c^j_{ph}(t)+\sum_{k=1}^{K}\alpha^j_{\lambda\mu k}(t)\langle p|Q_{\lambda\mu k}|h\rangle=i\frac{d}{dt}c^j_{ph}(t), \tag{12}$$

where ϵ_{ph} is the energy of a particle-hole excitation and $|p\rangle$ and $|h\rangle$ are particle and hole eigenstates of the static Hamiltonian (4). The collective amplitudes $\alpha^j_{\lambda\mu k}(t)$ and particle-hole contributions $c^j_{ph}(t)$ are expected to oscillate harmonically:

$$\alpha^j_{\lambda\mu k}(t)=\alpha^{j0}_{\lambda\mu k}\cos\omega t, \tag{13}$$

$$c^j_{ph}(t)=c^{j+}_{ph}e^{i\omega t}+c^{j-}_{ph}e^{-i\omega t}. \tag{14}$$

Substituting Eqs. (13) and (14) into Eq. (12) and collecting the coefficients of $e^{i\omega t}$ and $e^{-i\omega t}$, we obtain the connection

$$c^{j\pm}_{ph}=-\frac{1}{2}\frac{\Sigma_{k=1}^{K}\alpha^{j0}_{\lambda\mu k}\langle p|Q_{\lambda\mu k}|h\rangle}{\epsilon_{ph}\pm\omega}, \tag{15}$$

which expresses the particle-hole coefficients $c^{j\pm}_{ph}$ through the present unknown amplitudes $\alpha^{j0}_{\lambda\mu k}$.

To determine $\alpha^{j0}_{\lambda\mu k}$ we will consider the variation of the operator $Q_{\lambda\mu k}(\mathbf{r})$ in linear order. This can be written through the density variation

$$\delta Q_{\lambda\mu k}(t)=\int Q_{\lambda\mu k}(\mathbf{r})\,\delta n_j(\mathbf{r},t)d\mathbf{r}=-\sum_{k'=1}^{K}\alpha^j_{\lambda\mu k'}(t)\kappa^{-1}_{\lambda\mu kk'}, \tag{16}$$

where

$$\kappa^{-1}_{\lambda\mu kk'}=-\int Q_{\lambda\mu k}(\mathbf{r})[\nabla n_0(\mathbf{r})\nabla f_{\lambda\mu k'}(\mathbf{r})+n_0(\mathbf{r})\Delta f_{\lambda\mu k'}(\mathbf{r})]d\mathbf{r}. \tag{17}$$

An alternative expression is obtained using the wave function (11):

$$\delta Q_{\lambda\mu k}(t)=\left(\Psi^*_j(\mathbf{r}_1,\ldots,\mathbf{r}_{N_e},t)\left|\sum_{l=1}^{N_e}Q_{\lambda\mu k}(\mathbf{r}_l)\right|\times\Psi_j(\mathbf{r}_1,\ldots,\mathbf{r}_{N_e},t)\right)$$
$$=\sum_{ph}[c^{j*}_{ph}(t)\langle p|Q_{\lambda\mu k}|h\rangle+c^j_{ph}(t)\langle h|Q_{\lambda\mu k}|p\rangle]. \tag{18}$$

Equating expressions (16) and (18) and using Eqs. (13)–(15), one finally gets the system of homogeneous equations to determine the amplitudes $\alpha^{j0}_{\lambda\mu k}$:

$$\sum_{k'=1}^{K}S_{\lambda\mu kk'}(\omega)\alpha^{j0}_{\lambda\mu k'}=0, \tag{19}$$

with

$$S_{\lambda\mu kk'}(\omega)=\sum_{ph}\frac{\langle p|Q_{\lambda\mu k}|h\rangle\langle p|Q_{\lambda\mu k'}|h\rangle\epsilon_{ph}}{\epsilon^2_{ph}-\omega^2}-\frac{1}{2\kappa_{\lambda\mu kk'}}. \tag{20}$$

The condition

$$\det|S_{\lambda\mu kk'}(\omega)|=0 \tag{21}$$

provides nontrivial solutions to the system (19) and represents the SRPA dispersion equation for eigenenergies ω_j, where j is the number of the root of Eq. (21).

Equations (9), (15), (17), and (19)–(21) constitute the main points of the SRPA formalism: expressions for the self-consistent operators $Q_{\lambda\mu k}$, particle-hole coefficients $c^{j\pm}_{ph}$, strength constants $\kappa_{\lambda\mu kk'}$, collective amplitudes $\alpha^{j0}_{\lambda\mu k}$, and finally the dispersion equation.

It is worth making some additional comments on the SRPA formalism.

(i) The system (metal cluster) chooses *itself* the optimal contributions of the input local operators to every excited state j through the calculated amplitudes $\alpha^{j0}_{\lambda\mu k}$. The amplitudes are normalized as $\Sigma^K_{k=1}(\alpha^{j0}_{\lambda\mu k})^2=2$.

(ii) The rank of the determinant (21), being equal to the number of local operators, is much smaller than the rank of the matrices in the full RPA methods. At the same time, the total number of the roots is equal to the number of input particle-hole configurations and every excited state contains the same number of the particle-hole contributions. Thus the SRPA drastically simplifies the RPA calculations without losing an important RPA feature to describe the Landau damping.

(iii) In the case of one local operator, the dispersion equation (21) is reduced to the well-known equation [25,27]

$$S_{\lambda\mu}(\omega)=0. \tag{22}$$

Just the same dispersion equation would take place if we start with the Hamiltonian containing the separable residual interaction

$$H_{\lambda\mu}=H_0-\tfrac{1}{2}\,\kappa_{\lambda\mu}Q^{\dagger}_{\lambda\mu}Q_{\lambda\mu}. \tag{23}$$

It may also be shown that in the general case of many local operators, the dispersion equation (21) is quite similar (but, due to the self-consistency, does not coincide exactly) to the one obtained with a more general separable interaction

$$H_{\lambda\mu}=H_0-\frac{1}{2}\sum_{k,k'=1}^{K}\kappa_{\lambda\mu kk'}Q^{\dagger}_{\lambda\mu k}Q_{\lambda\mu k'}. \tag{24}$$

It is easy to see that the values $\kappa_{\lambda\mu kk'}$ have the physical meaning of strength constants of the residual forces (9). If more than one local operator is used, the nondiagonal strength constants take place. Our calculations have shown that these constants are of the same order of magnitude as the diagonal ones. Nondiagonal strength constants play an important role: They regulate in a self-consistent way the Hamiltonian after adding a new interaction.

(iv) Neglecting the direct Coulomb terms in the SRPA, one gets the model for the self-consistent description of isoscalar collective excitations (giant resonances) in atomic nuclei. This model operates with density-dependent residual forces. Further, assuming for the single-particle potential the ansatz $V(\mathbf{r})=(dv/dn)_{n=n_0}$ and using only one local operator with $p_k=\lambda$, we obtain equations of the familiar vibrating potential model, which is widely used in nuclear physics (see [25,26,29,46] and references therein). Quite recently this model was successfully applied for the description of isoscalar $E\lambda$ giant resonances in deformed and superdeformed nuclei [29].

III. RESULTS AND DISCUSSION

The Kohn-Sham with sharp and diffused jellium and Woods-Saxon single-particle schemes were used for calculation of the single-particle wave functions and energies. For both neutral and charged clusters, we used the same parameters of the Kohn-Sham jellium, namely, $r_{WS}=3.96$ a.u.$=2.09$ Å and $a_0=1$a.u.$=0.529$ Å ($a_0=0$ for sharp jellium) [42]. Following the prescription of Gunnarsson and Lundqvist [44], the expression for the exchange-correlation term in the ground state has the form (in atomic units 1a.u.$=2$ Ry$=27.2$ eV for energies and 1a.u.$=0.529$ Å for lengths)

$$v(n_0(\mathbf{r}))=\frac{1}{2}n_0(\mathbf{r})\left[-\frac{3}{2}\left(\frac{9}{4\pi^2}\right)^{1/3}\frac{1}{r_s(\mathbf{r})}-0.0666G\left(\frac{r_s(\mathbf{r})}{11.4}\right)\right], \tag{25}$$

where $r_s(\mathbf{r})=[3/4\pi n_0(\mathbf{r})]^{1/3}$ and

$$G(x)=(1+x^3)\ln\left(1+\frac{1}{x}\right)-x^2+\frac{x}{2}-\frac{1}{3}. \tag{26}$$

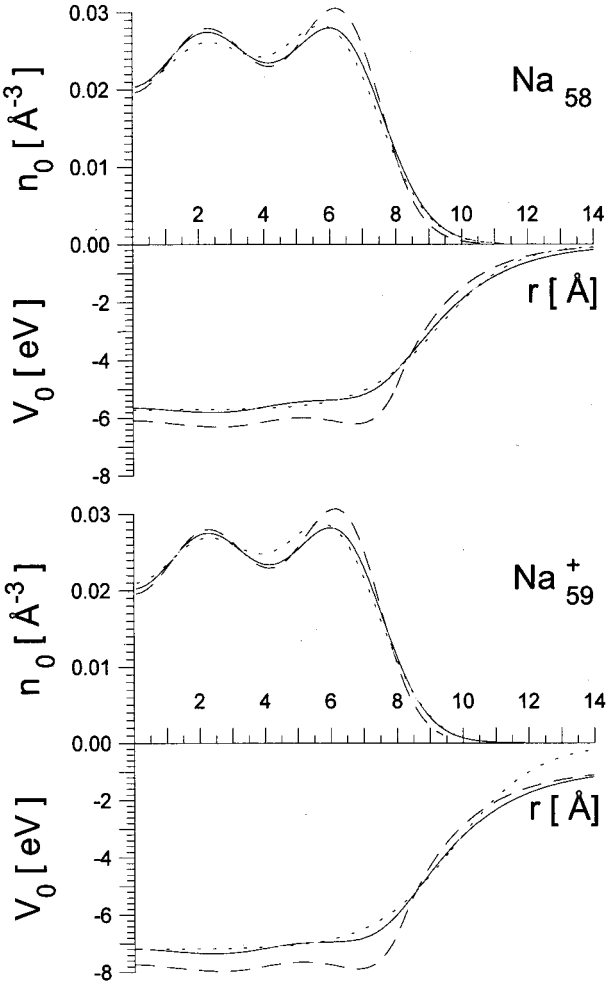

FIG. 1. Ground-state densities $n_0(r)$ and single-particle potentials $V_0(r)$ in Na_{58} and Na_{59}^{+} calculated with the diffused Kohn-Sham (solid line), sharp Kohn-Sham (dashed line), and Woods-Saxon (dotted line) single-particle schemes.

It is worth noting that the self-consistent residual forces (9) are mainly determined by direct Coulomb interaction, while the exchange-correlation effects play a minor role.

The parameters of the Woods-Saxon potential were adjusted so as to reproduce on average the diffused Kohn-Sham ground-state densities in a wide region. The fit yielded $r_0=2.4$ Å, $V_0=-5.7$ eV, and $a_0=1.11$ Å for neutral clusters and $r_0=2.5$ Å, $V_0=-7.2$ eV, and $a_0=1.25$ Å for singly charged clusters. They are somewhat different from the parameters $r_0=2.25$ Å, $V_0=-6$ eV, and $a_0=0.74$ Å, proposed in [47] for neutral clusters. These latter values lead to overestimation of the plasmon energy and high-energy strength. As seen from Fig. 1, we have succeeded in getting a nice fit of the Woods-Saxon densities even for the case of charged clusters whose Kohn-Sham potential deviates considerably from the Woods-Saxon form in the surface region and beyond. As will be noticed from Fig. 3, the Woods-Saxon potential with the above parameters provides almost the same SRPA results as the Kohn-Sham scheme.

Two main kinds of the SRPA calculations are presented: with and without coupling of surface modes with volume

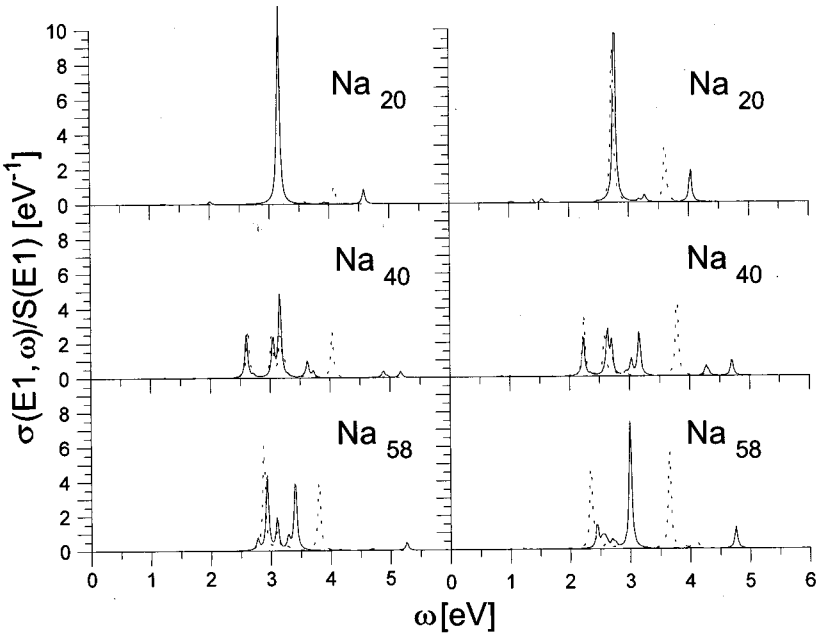

FIG. 2. $E1$ strength functions calculated with (solid line) and without (dotted line) coupling with volume modes. The results obtained with the diffused (sharp) Kohn-Sham are given on the right- (left-) hand side.

ones. In the first case, the sets of four local operators $f_{\lambda\mu k}(\mathbf{r})$ mentioned in Sec. II are used. In the second case, only the operators with $p_k=\lambda$ are taken into account, i.e., volume modes are neglected. The results of calculations are presented in the form of the normalized strength function

$$\sigma(E\lambda,\omega)=\frac{1}{S(E\lambda)}\sum_j \omega_j B(E\lambda,gr\rightarrow\omega_j)\rho(\omega-\omega_j), \qquad (27)$$

where

$$\rho(\omega-\omega_j)=\frac{1}{2\pi}\frac{\Delta}{(\omega-\omega_j)^2+(\Delta/2)^2} \qquad (28)$$

is the weight function with the averaging parameter $\Delta=0.05$ eV, $B(E\lambda,gr\rightarrow\omega_j)$ is the reduced probability of the $E\lambda$ transition from the ground state to the one-phonon state with the excitation energy ω_j, and $S(E\lambda)$ is the energy-weighted sum rule

$$S(E\lambda)=\sum_j \omega_j B(E\lambda,gr\rightarrow\omega_j)$$
$$=\frac{\hbar^2e^2}{8\pi m_e}\lambda(2\lambda+1)^2N_e\langle r^{2\lambda-2}\rangle. \qquad (29)$$

Expression (27) has a form similar to the photoabsorption cross section for dipole excitations. However, this is not exactly the photoabsorption cross section, but only the convenient form of presentation of the RPA results where the values $\omega_j B(E\lambda,gr\rightarrow\omega_j)$ are slightly averaged to avoid unnecessary details.

Let us consider results of the calculations. Figure 2 shows that jellium diffuseness leads to a considerable redshift of the plasmon energy and thus improves the agreement with the experimental data. If only the divergency-free operator ($p_k=1$) is used, the calculations give rather strong high-energy peaks at 3.5–4.5 eV in both cases of diffused and sharp jellium. The analysis of associated transition densities shows that these peaks are partly of a volume character. A similar result has been obtained in Ref. [16]. At the same time, the experiments [20–23] do not support such a strong high-energy strength. The description is improved if the coupling with volume modes is taken into account ($p_k=1,4,7,10$). Then the main part of the high-energy strength is strongly redshifted and the dipole strength is mainly concentrated in the surface plasmon region 2.5–3.3 eV. A smaller part of the high-energy strength is blueshifted to about the region of the volume plasmon where it is strongly fragmented. Such a redistribution of the strength considerably improves the description of the static dipole polarizability.

The main SRPA results for dipole excitations, obtained with the coupling of surface and volume modes, are presented in Figs. 3 and 4 and Table I. Figure 3 and Table I show that surface plasmon energies in charged clusters are slightly blueshifted compared to the energies in neutral ones, which is observed experimentally. In agreement with the measurements [23], the calculated energies of main plasmon peaks in charged clusters decrease with a cluster size until $N_e=40$ and then increase for larger clusters. If the RPA peaks are averaged with $\Delta=0.25$ eV, which roughly corresponds to experimental widths, it is easy to see that, except for $N_e=40$ and 58, a one-peak structure of the plasmon is obtained. A resonance right-hand shoulder observed in [23] for charged clusters with $N_e=20,40,58$, and 92 is reproduced for $N_e=20$ and 40 and not for $N_e=58$ and 92. The discrepancies are partly caused by the highest single-particle levels (with the energies about zero), which, being very sensitive to the details of the calculations, influence noticeably the gross structure of the plasmon in $N_e=40,58$, and 92 clusters.

For clusters with $N_e=40$, 58, 92, and 138 the calculations give a considerable Landau damping that could determine to a large extent the plasmon width. In agreement with the discrete-matrix RPA results [10], the fragmentation of the dipole strength is increased with the size from $N_e=8$ to 40, reaching the maximal value at $N_e=40$. Then the frag

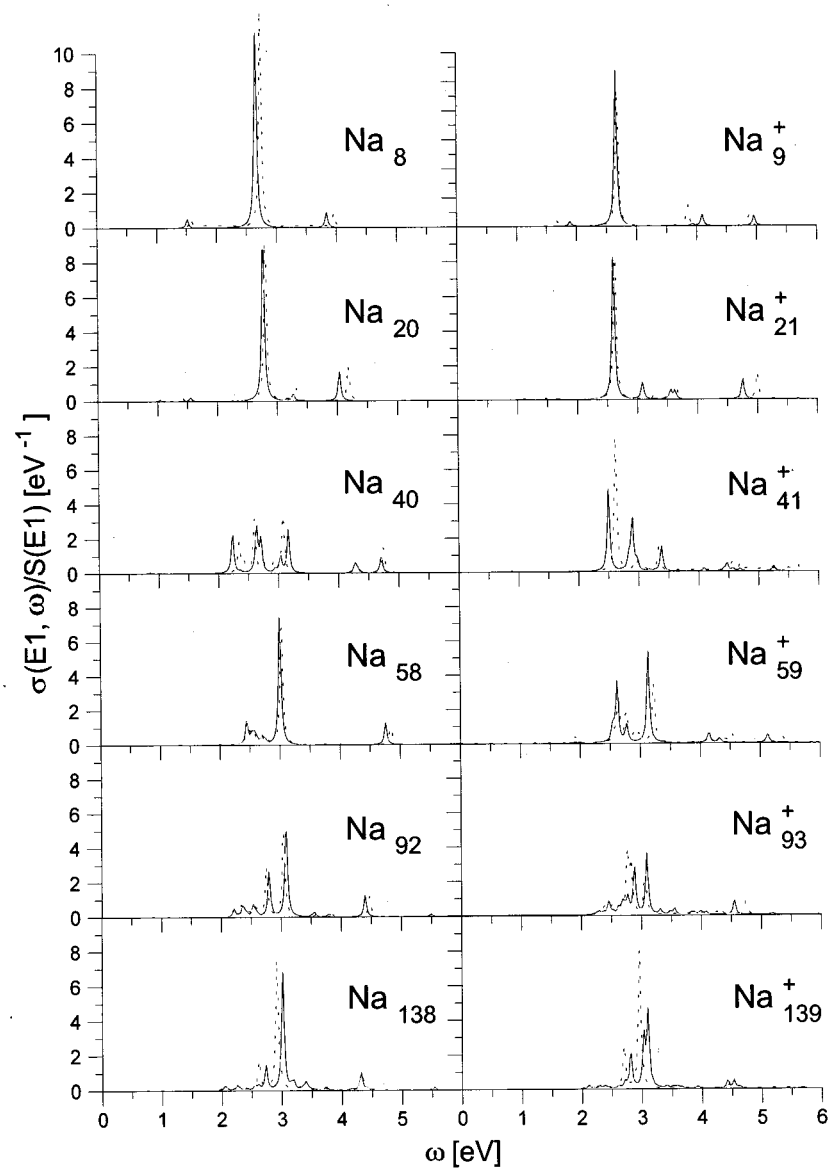

FIG. 3. $E1$ strength functions calculated taking into account coupling with volume modes. The diffused Kohn-Sham (solid line) and Woods Saxon (dotted line) single-particle schemes are used.

mentation gradually decreases with the size. These tendencies have been explained in [10] as a result of the degeneracy of the original (before the breakup) plasmon with neighboring particle-hole configurations. Just for Na_{40}, the original plasmon, comprising mainly $\Delta N=1$ (N is the principle shell quantum number) transitions, has the position in the neighborhood of the $\Delta N=3$ transitions, which provides the most optimal conditions for the fragmentation of the dipole strength. In general, the extent of the plasmon fragmentation obtained within the SRPA agrees well with the full RPA results [10]. The SPRA results for charged clusters do not reproduce the experimental trend of the plasmon width to decrease with a cluster size until $N_e=40$ and then to increase again for larger clusters [23]. This discrepancy is most probably caused by neglecting temperature fluctuations that are known to determine to a large extent plasmon widths in spherical clusters. The calculated Landau damping, providing only a part of the plasmon width (up to $10-20\,\%$ in $N_e=8$ and 20 and larger in bigger clusters), seems not to be enough to reproduce the trend [23].

In Fig. 4 the results for very large singly charged clusters are presented. In spite of quite extended configuration space used for these cluster, the SRPA calculations need a little computer effort. Figure 4 clearly shows the approaching of the dipole plasmon to the classical Mie result ($\omega_{Mie}=\omega_p/\sqrt{3}=3.41$ eV for sodium) with a large cluster size.

Table I shows that, in general, the calculated plasmon energies are in a quite acceptable agreement with the experimental data. While comparing the theory with the experiment, one should take into account that for $N_e\geqslant 40$ the calculated energy *centroids* are presented against the experimental *main peak* positions. It seems to be a main reason of the ''overestimation'' of plasmon energies for charged clusters with $N_e\geqslant 40$. Indeed, the experimental centroid energies involving a strong right-hand shoulder should be larger than the corresponding energies of main peaks and thus be closer to the theoretical values. Starting with $N_e=40$, the general tendency of increasing plasmon energy with a cluster size is reproduced. A good description of the

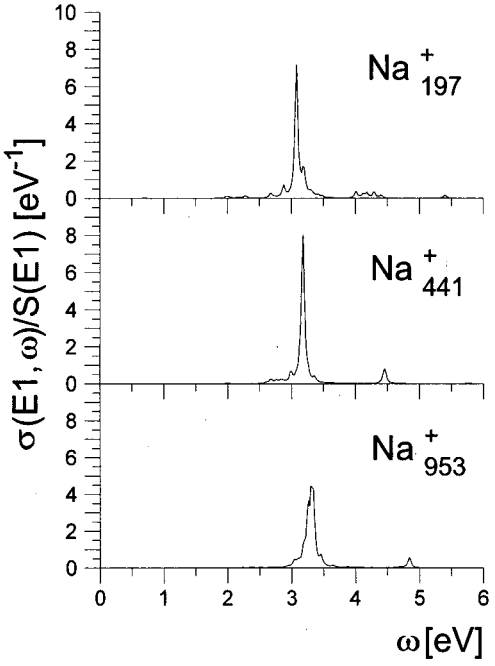

FIG. 4. $E1$ strength functions for large singly charged clusters. The calculated diffused Kohn-Sham single-particle scheme is used and coupling with volume modes is taken into account.

TABLE I. Dipole plasmon energies $\overline{\omega}$ (centroids for $N_e \geq 40$) and static dipole polarizabilities ϱ (in units R^3 with $R = r_{WS} N_e^{1/3}$, $r_{WS} = 3.96$ a.u.).

	$\overline{\omega}$(eV)		$\varrho(R^3)$	
Cluster	Expt.	SRPA	Expt.	SRPA
Na_8	2.59 [a]	2.66	1.77 [a]	1.78
Na_{20}	2.67 [a]	2.80	1.67 [a]	1.57
Na_{40}	2.72 [a]	2.68	1.62 [a]	1.64
Na_{58}		2.83		1.41
Na_{92}		2.85		1.41
Na_{138}		2.91		1.37
Na_9^+	2.71 [b]	2.66		1.44
Na_{21}^+	2.68, [b] 2.68(1) [c]	2.61		1.51
Na_{41}^+	2.60, [b] 2.62(1) [c]	2.75		1.51
Na_{59}^+	2.70 [b]	2.85		1.39
Na_{93}^+	2.75 [b]	2.88		1.36
Na_{139}^+		2.94		1.34
Na_{197}^+		3.09		1.27
Na_{441}^+		3.18		1.16
Na_{953}^+		3.28		1.18

[a]Reference [20].
[b]The experimental values are extracted from figures of Ref. [23].
[c]Reference [21].

static dipole polarizability $\varrho = \Sigma_j \omega_j^{-1} B(E\lambda, gr \rightarrow \omega_j)$ is also achieved and the correct trend of this value to unity with a cluster size is exhibited. It should be noted that the appropriate energy positions of the main plasmon peaks have been mainly obtained due to the diffuseness of the ionic jellium. As for the coupling with volume modes, its role mainly consists in the considerable redshift of the high-energy strength. The calculations of the collective amplitudes $\alpha^{j0}_{\lambda\mu k}$ show that the main plasmon peaks are dominated by the divergency-free operator with $p_k = 1$ and only high-energy peaks have considerable contributions from the operators with $p_k > 1$. This means that the system, in spite of the proposed freedom to develop collective oscillations through volume collective modes, tends to have a dipole plasmon of mainly surface character. Finally, the SRPA results (surface plasmon energies, extent of fragmentation, static dipole polarizabilities, and main tendencies with a cluster size) seem not to be worse than the results obtained within the local RPA [19,24,35] or full RPA [6–12,32], which confirms the validity of the separable ansatz for the description of dipole excitations in sodium clusters. Few deviations from the experimental data and general tendencies, which take place for

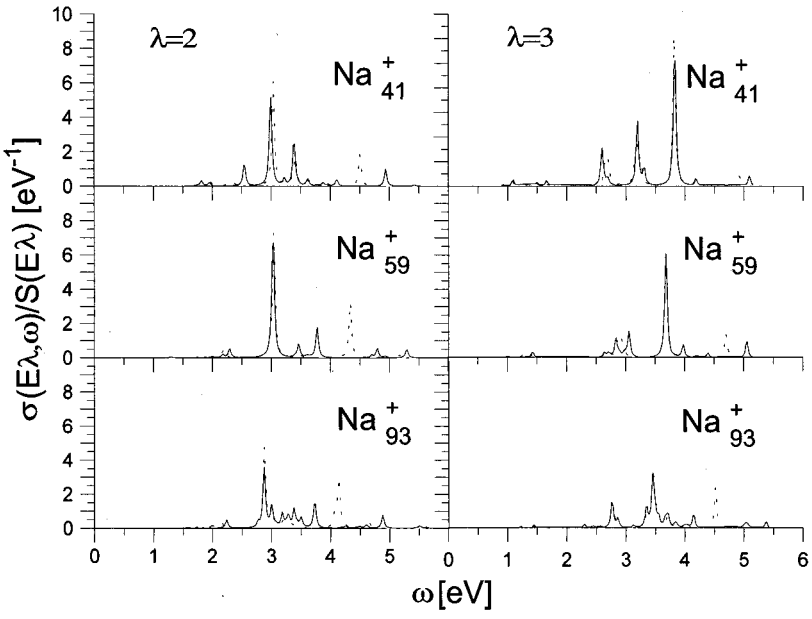

FIG. 5. $E2$ and $E3$ strength functions calculated with (solid line) and without (dotted line) coupling with volume modes. The diffused Kohn-Sham is used.

small and very large clusters (e.g., the plasmon energy and ϱ for Na_{20} as well as the ϱ for Na_{953}^{+}), can be explained by using in the present calculations the same parameters of the Kohn-Sham single-particle scheme for neutral (charged) clusters in a very wide region.

Figure 5 exhibits the SRPA results for $E2$ and $E3$ collective oscillations in singly charged clusters. It is seen that $E2$ and $E3$ strengths are mainly concentrated in the energy regions 2.5–3.5 and 3–4 eV, respectively. Main peaks are well pronounced and lie below the continuum threshold. The decreasing in the $E2$ and $E3$ resonance energies with a size takes place in agreement with the sum-rule results [18]. Like in the dipole case, the coupling with volume modes noticeably leads to a redshift of the high-energy $E2$ and $E3$ strength.

IV. CONCLUSION

The self-consistent schematic RPA is generalized to take into account the coupling of different kinds of collective motion. The method exploits the separable ansatz for the residual interaction that drastically simplifies the RPA calculations without losing such an essential RPA property as the description of the Landau damping of the collective strength. The SRPA is applied to the description of dipole oscillations in spherical sodium clusters with taking into account the coupling of surface and volume dipole modes. Good agreement with the experimental data (dipole plasmon energies, Landau damping, static dipole polarizabilities, and main tendencies with increasing a cluster size) in a wide region is achieved. In particular, the excess of the high-energy dipole strength obtained in previous SRPA calculations [16] is removed. Finally, one may conclude that the present study proves the validity of the separable approximation to the RPA description of the dipole collective strength in sodium clusters. The main applications of the method are expected for deformed and very large clusters where we are forced to use an extended configuration space. It would be interesting to test the applicability of the separable ansatz for clusters with a considerable coupling of valence electrons with ions as well as for molecules.

The RPA predictions for $E2$ and $E3$ collective oscillations are also given. Different sets of Woods-Saxon parameters providing a good description of the surface dipole plasmon are proposed for neutral and singly charged sodium clusters.

ACKNOWLEDGMENTS

We are grateful to M. Brack, P.-G. Reinhard, and Th. Hirschmann for numerous fruitful discussions and providing the code for the Kohn-Sham single-particle scheme in spherical clusters. The work was partly supported by INTAS Grant No. 0151 (V.O.N. and V.V.G.) and an INFN grant (V.O.N.)

[1] V. V. Kresin, Phys. Rep. **220**, 1 (1992).
[2] V. O. Nesterenko, Sov. J. Part. Nucl. **23**, 1665 (1992).
[3] W. A. de Heer, Rev. Mod. Phys. **65**, 611 (1993).
[4] M. Brack, Rev. Mod. Phys. **65**, 677 (1993).
[5] C. Brechignacand J. P. Connerade, J. Phys. B **27**, 3795 (1994).
[6] W. Ekardt, Phys. Rev. B **31**, 6360 (1985).
[7] J. M. Pachecoand W. Ekardt, Ann. Phys. (Leipzig) **1**, 254 (1992).
[8] W. Ekardtand Z. Peznar, Phys. Rev. B **43**, 1322 (1991).
[9] D. E. Beck, Phys. Rev. B **35**, 7325 (1987); **43**, 7301 (1991).
[10] C. Yannouleas, E. Vigezzi, and R.f A. Broglia, Phys. Rev. B **47**, 9849 (1993).
[11] C. Yannouleas, F. Catara, and N. Van Giai, Phys. Rev. B **51**, 4569 (1995).
[12] M. Madjet, C. Guet, and W. R. Johnson, Phys. Rev. A **51**, 1327 (1995).
[13] E. Lipparinand S. Stringari, Z. Phys. D **18**, 193 (1991).
[14] P.-G. Reinhardand Y. K. Gambhir, Ann. Phys. (Leipzig) **1**, 598 (1992); P.-G. Reinhard, *ibid.* **1**, 632 (1992).
[15] V. O. Nesterenkoand W. Kleinig, Phys. Scr. **T56**, 284 (1995).
[16] V. O. Nesterenko, W. Kleining, and V. V. Gudkov, Z. Phys. D **34**, 271 (1995).
[17] E. Lipparinand S. Stringari, Phys. Rep. **175**, 104 (1989).
[18] Ll. Serra, F. Garcias, M. Barranko, J. Navarro, C. Balbias, and A. Mananes, Phys. Rev. B **39**, 8247 (1989).
[19] P.-G. Reinhard, M. Brack, and O. Genzken, Phys. Rev. A **41**, 5568 (1990).
[20] K. Selby, M. Vollmer, J. Masui, V. Kresin, W. A. de Heer, and W. D. Knight, Phys. Rev. B **40**, 5417 (1989).
[21] J. Borgreen, P. Chowdhury, N. Kebaili, L. Lundsberg-Nielsen, K. Lutzenkirchen, M. B. Nielsen, J. Pedersen, and H. D. Rasmussen, Phys. Rev. B **48**, 17 507 (1993).
[22] C. Brechignac, P. Cahuzak, F. Carlier, M. de Frutos, and J. Leygneir, Z. Phys. D **19**, 1 (1991).
[23] Th. Reiners, Ch. Ellert, M. Schmidt, and H. Haberland, Phys. Rev. Lett. **74**, 1558 (1995).
[24] M. Brack, Phys. Rev. B **39**, 3533 (1989).
[25] D. J. Rowe, *Nuclear Collective Motion* (Methuen, London, 1970), Chaps. 4 and 14–16.
[26] A. Bohr and B. Mottelson, *Nuclear Structure* (Benjamin, New York, 1974), Vol. II, Chap. 6.
[27] P. Ring and P. Schuck, *The Nuclear Many-Body Problem* (Springer-Verlag, Heidelberg, 1980), Chaps. 8 and 12.
[28] V. G. Soloviev, *Theory of Atomic Nuclei: Quasiparticles and Phonons* (Institute of Physics, Bristol, 1992).
[29] V. O. Nesterenko, W. Kleinig, V. V. Gudkov, and J. Kvasil, Phys. Rev. C **53**, 1632 (1996).
[30] V. O. Nesterenko and W. Kleinig (unpublished).
[31] J. Borgreen (private communication); M. Schmidt and H. Haberland (private communication).
[32] P.-G. Reinhard (private communication).
[33] V. O. Nesterenko, in *Proceedings of the Second International Conference on Atomic and Nuclear Clusters, Santorini, Greece, 1993*, edited by G. S. Anagnostatos and W. von Oertzen (Springer-Verlag, Berlin, 1994), p. 256.
[34] P. Meibom, M. Østergård, J. Borggreen, B. Bjørnholm, and H.

D. Rasmussen, Proceedings of the Eighth International Symposium on Small Particles and Inorganic Clusters, Copenhagen, 1996 [Z. Phys. D (to be published)].
[35] M. Brack and Th. Hirschmann (private communication).
[36] V. O. Nesterenko, W. Kleinig, V. V. Gudkov, N. Lo Iudice, and J. Kvasil (unpublished).
[37] P.-G. Reinhard, S. Weisberger, O. Genzken, and M. Brack, Lect. Notes Phys. **404**, 254 (1992).
[38] H. Steinwedel and J. H. D. Jensen, Z. Naturforsch. Teil A **5**, 413 (1950).
[39] M. Goldhaber and E. Teller, Phys. Rev. **74**, 1046 (1948).
[40] W. D. Myers, W. J. Swiatecki, T. Kodama, L. J. El-Jaik, and E. R. Hilf, Phys. Rev. C **15**, 2032 (1977).
[41] S. V. Tolokonnikov and S. A. Fayans, Pis'ma Zh. Éksp. Teor. Fiz. **35**, 403 (1982) [JETP Lett. **35**, 499 (1982)].
[42] Th. Hirschmann, M. Brack, and J. Mejer, Ann. Phys. (Leipzig) **3**, 336 (1994).
[43] Th. Hirschmann, B. Montag, and J. Mejer, Z. Phys. D **37**, 63 (1996).
[44] O. Gunnarson and B. I. Lundqvist, Phys. Rev. B **13**, 4274 (1974).
[45] D. J. Thouless, Nucl. Phys. **21**, 225 (1960).
[46] E. Lipparini and S. Stringari, Nucl. Phys. A **371**, 445 (1981).
[47] H. Nishioka, K. Hamen, and B. R. Mottelson, Phys. Rev. B **42**, 9377 (1990).